Validation of a Spatially Interconnected Model for Flow Transition Control

Saulat S. Chughtai, Gabriela Rusnáková, Herbert Werner, Mária Lukáčová

***Abstract*— A novel linearized model for the transition control problem in plane Poiseuille flow has been proposed recently. The model is based on a finite difference approach in streamwise direction and a spectral approach in wall normal direction. It is thus valid for all spatial frequencies and can be used for the synthesis of controllers for flow control problems, using recently developed ideas for spatially interconnected systems. In this paper this model is validated in both time and frequency domain. For time domain validation, the transient energy is calculated and compared with previously published results. The frequency domain validation is based on nonlinear simulation: a sinusoidal disturbance is applied at the lower boundary and its effect at different locations of the channel are simulated. From a Fourier analysis of the simulated responses, the spatial and temporal frequency responses are obtained and compared with the linearized model. The results suggest that the model captures the dominant features of the problem and can be used for the design of spatially interconnected controllers.**

I. Introduction

In many engineering applications the process of laminar-turbulence transition in plane Poiseuille flow is of particular importance. Laminar flow exhibits less drag and heat transfer, whereas turbulent flow is required for thorough mixing. However, the use of linear control theory for controlling flow instabilities, which cause the transition, is a fairly new approach. Earlier work related to this field mostly concentrated on superimposing anti-phase modes to cancel sinusoidal disturbances.

The underlying control scheme has an array of sensors which measure stream-wise and span-wise skin friction. The actuators are mounted on the walls which can change the boundary condition on the wall normal component of velocity. A detailed exposition of the problem can be found in [1].

In order to synthesize a controller for flow transition using modern control techniques, a mathematical model is required. The dynamical behavior of laminar flow are governed by the Navier-stokes equation (NSE), which are nonlinear coupled partial differential equations. In order to model the transition from laminar to turbulent flow, these are linearized around the laminar flow. Spectral methods [2] are then used to approximate the dynamics of the system for a particular spatial frequency and time evolution of velocities away from boundaries. In [3] a new model has been proposed where a finite difference scheme is used in flow direction, and modified Chebyshev polynomials are used in wall normal direction. This model is not restricted to a single spatial frequency, and can be used to design controllers in physical domain rather then Fourier domain, in contrast to previously presented models.

In this paper, the model presented in [3] is validated in both time and frequency domain. In flow transition problems, the normality of eigenvectors is an important property, as discussed in [4], [5], and a suitable measure for this is transient energy defined in [4], [6]. For time domain validation we have used transient energy. It is shown that the transient energy response of the linearized model captures the dominant features of the nonlinear model. For frequency domain analysis first the linearized model is used to generate the frequency responses at different locations of the channel. These are then validated against a nonlinear simulation of the plane Poiseuille flow. A Fourier transform of the responses obtained in nonlinear simulations, reveals that even if the amplitude of input disturbance is less than 10% of the channel width, nonlinear effects may dominate. This observation is in agreement with the results obtained by [7]. Furthermore, the frequency responses obtained from these nonlinear simulations are compared with the frequency responses of the linearized model presented in [3].

The paper is organized as follows: In section 2 the linearized model of [3] is reviewed. Section 3 deals with time domain validation, where relations for transient energy are derived and used to validate the response of the proposed linearized model. Section 4 presents details of the nonlinear simulation and a comparison between the frequency domain responses of the linearized and nonlinear model, using the Fourier transform. In the last section conclusions are drawn and some future research directions are presented.

II. Finite Difference Model

Consider a two-dimensional steady state plane channel flow with maximum velocity U_0 and channel half-width δ as shown in Fig 1.

The standard NSE can be linearized by first normalizing all velocities about the centreline velocity U_0 and half height δ. Then, assuming laminar flow, the NSE can be linearized around the mean velocity profile in the streamwise direction (x). For laminar flow the mean velocity profile can be written as $U(y) = 1 - y^2$ on the domain $y \in [-1, 1]$. The equation governing small, incompressible, three-dimensional perturbations $\{u, v, p\}$ are then given by the linearized NSE

S. S. Chughtai and H. Werner are with the Institute of Control Systems, Hamburg University of Technology, 21073 Hamburg, Germany {saulat.chughtai, h.werner}@tu-harburg.de

G. Rusnáková and M. Lukáčová are with the Institute for Numerical Simulation, Hamburg University of Technology, 21073 Hamburg, Germany

$$\left\{(S_1+S_1^{-1}-2)I_{N+1}\Gamma+\Gamma''\right\}\dot{a}+\dot{q}b_1 = qb_2-\frac{U}{2}(S_1^2-2S_1+2S_1^{-1}-S_1^{-2})I_{N+1}\Gamma a - U(S_1-S_1^{-1})I_{N+1}\frac{1}{2}\Gamma'' a+\frac{d^2U}{dy^2}(S_1-S_1^{-1})I_{N+1}\frac{1}{2}\Gamma a + \frac{1}{Re}(S_1^2-4S_1-4S_1^{-1}+S_1^{-2}+6)\Gamma a + \frac{2}{Re}(S_1+S_1^{-1}-2)I_{N+1}\Gamma'' a+\frac{1}{Re}\Gamma'''' a \quad (12)$$

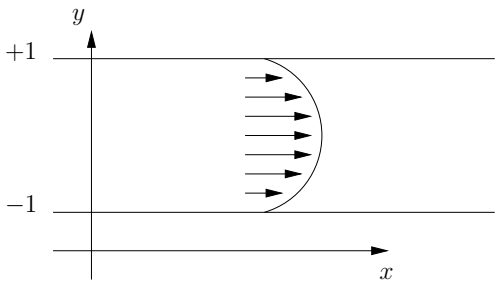

Fig. 1. Plane Poiseuille flow, 2D case

and the continuity equations,

$$\begin{aligned}\frac{\partial u}{\partial t}+U\frac{\partial}{\partial x}u+\frac{dU}{dy}v &= -\frac{\partial p}{\partial x}+\frac{1}{Re}\Delta u\\ \frac{\partial v}{\partial t}+U\frac{\partial}{\partial x}v &= -\frac{\partial p}{\partial y}+\frac{1}{Re}\Delta v\\ \frac{\partial u}{\partial x}+\frac{\partial v}{\partial y} &= 0\end{aligned} \quad (1)$$

where $\Delta \equiv \partial^2/\partial x^2+\partial^2/\partial y^2$ and Re is the Reynolds number, u and v are velocities in x and y-directions and p is the pressure. The set of equations (1) forms a system of three linear partial differential equations in three flow variables (u,v,p). These can be converted to a velocity-vorticity formulation, which in the 2-dimensional case is given as, [8],

$$\Delta\dot{v} = \left\{-U\frac{\partial}{\partial x}\Delta+\frac{d^2U}{dy^2}\frac{\partial}{\partial x}+\frac{\Delta^2}{Re}\right\}v \quad (2)$$

with homogeneous boundary conditions

$$v(x,y=\pm1,t) = 0 \quad (3)$$

$$\frac{\partial v(x,y=\pm1,t)}{\partial y} = 0 \quad (4)$$

Using a change of variables, control inputs can be introduced, [9]. For this, let us consider

$$v(x,y,t) = \phi(x,y,t)+q(t)w(x)f(y) \quad (5)$$

where the function $w(x)$ is a weighting (it represents the effect of control action along x-direction). The function $f(y)$ represents the effect of boundary control on the wall normal velocity profile at location y. In terms of the new variable ϕ the modified boundary value partial differential equation is given as

$$\Delta\dot{\phi}+\dot{q}\Delta(wf) = -qU\frac{\partial}{\partial x}\Delta(wf)+qf\frac{d^2U}{dy^2}\frac{\partial w}{\partial x} + q\frac{\Delta^2}{Re}(wf)-U\frac{\partial}{\partial x}\Delta\phi + \frac{d^2U}{dy^2}\frac{\partial\phi}{\partial x}+\frac{\Delta^2}{Re}\phi \quad (6)$$

with the Neumann and Dirichlet (ND) boundary conditions given as

$$\phi(x,y=\pm1,t)=0, \qquad \frac{\partial\phi(x,y=\pm1,t)}{\partial y}=0 \quad (7)$$

Using the approach of [3], (6) can be expressed in spatially interconnected form. For this let us define

$$a = \begin{bmatrix}a_4\\ \vdots\\ a_N\end{bmatrix} \quad (8)$$

$$\Gamma = \begin{bmatrix}\Gamma_4(y_2) & \dots & \Gamma_N(y_2)\\ \vdots & \vdots & \vdots\\ \Gamma_4(y_{N-2}) & \dots & \Gamma_N(y_{N-2})\end{bmatrix} \quad (9)$$

$$\Gamma' = \begin{bmatrix}\frac{\partial\Gamma_4}{\partial y}|_{y_2} & \dots & \frac{\partial\Gamma_N}{\partial y}|_{y_2}\\ \vdots & \vdots & \vdots\\ \frac{\partial\Gamma_4}{\partial y}|_{y_{N-2}} & \dots & \frac{\partial\Gamma_N}{\partial y}|_{y_{N-2}}\end{bmatrix} \quad (10)$$

$$b_1 = \begin{bmatrix}\frac{\partial^2 f}{\partial y^2}|_{y_2}\\ \vdots\\ \frac{\partial^2 f}{\partial y^2}|_{y_{N-2}}\end{bmatrix} \quad b_2 = \begin{bmatrix}\frac{1}{Re}\frac{\partial^4 f}{\partial y^4}|_{y_2}\\ \vdots\\ \frac{1}{Re}\frac{\partial^4 f}{\partial y^4}|_{y_N}\end{bmatrix} \quad (11)$$

where $\Gamma_i(y_k)$ and a_i are the i^{th} Chebyshev polynomial, evaluated at $y_k=\cos(\pi k/N)$, and its coefficients. Similarly we define Γ'' and Γ''''. Then, we can write (6) in matrix form as (12), where S and S^{-1} represent the spatial forward shift and backward shift operator, respectively.

III. Time Domain Validation

In [5] it is proposed that the phenomenon of transition from laminar flow to turbulence in plane Poiseuille flow is due the non-normality of the eigenvectors of adjacent eigenvalues. This non-normality causes an initial increase in the impulse response of a system. It is further shown in [10] that for a linear system $\dot{x}=Ax$, where A is stable and $\alpha(A)$ is its spectral abscissa, we have $||exp(At)|| = e^{t\alpha}$, if A is normal.

If it is not normal then

$$e^{t\alpha} \leq ||exp(tA)|| \leq \kappa(V)e^{At}, \quad \forall t \geq 0$$

where $\kappa(V)$ is the condition number of the matrix of eigenvectors of A. Thus, a non-normal stable system will display a larger peak in the impulse response before exponential decaying to zero. It is argued in [5] that due to this peak, the linearized model displays a flow transition at a Reynolds number much smaller than $Re = 5772$. In [4] the authors have used the concept of transient energy or energy density to assess the non-normality of plane Poiseuille flow. In this section we will compare the transient energy growth $(E(t))$ of the linearized model (12) with $E_s(t)$ obtained by [6].

A. Transient Energy of Finite Difference Model

Consider a single element of the channel as shown in Fig. 2. The transient energy is defined as [4],

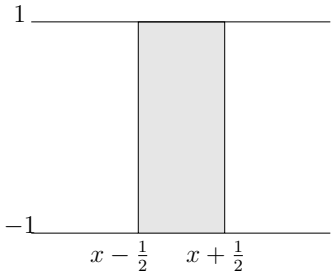

Fig. 2. Single element of a channel, 2D case

$$E(t) = \frac{1}{2V}\int_{-1}^{1}\int_{-\frac{1}{2}}^{\frac{1}{2}} \frac{u^2+v^2}{2} dxdy \tag{13}$$

where unit mass density of the fluid is assumed. Since $V = 2$ and both v and $\frac{dv}{dy}$ are assumed to remain constant in x-direction in the single element, we obtain using the continuity equation

$$E(t) = \frac{1}{4}\int_{-1}^{1} v^2 - (\frac{\partial v}{\partial y})^2 dy \tag{14}$$

Now we can approximate an integral by a weighted sum as [9],

$$\begin{aligned} \int_{-1}^{1} v^2 dy &= \sum_{n=0}^{N} w_n v(y_n), \\ \int_{-1}^{1} (\frac{\partial v}{\partial y})^2 dy &= \sum_{n=0}^{N} w_n (\frac{\partial v}{\partial y}\Big|_{y_n})^2. \end{aligned} \tag{15}$$

where $\forall n = 1, N-1$

$$w_n = \frac{2}{N}\sqrt{1-y_n^2}\sum_{m=1}^{N-1}\frac{1}{m}\sin(m\pi n/N)(1-\cos(m\pi)) \tag{16}$$

and $w_0 = w_N = 0$. Putting (15) in (14) and arranging the terms in matrices we obtain

$$E(t) = \frac{\Lambda^T\Psi\Lambda - \Lambda_y^T\Psi\Lambda_y}{4} \tag{17}$$

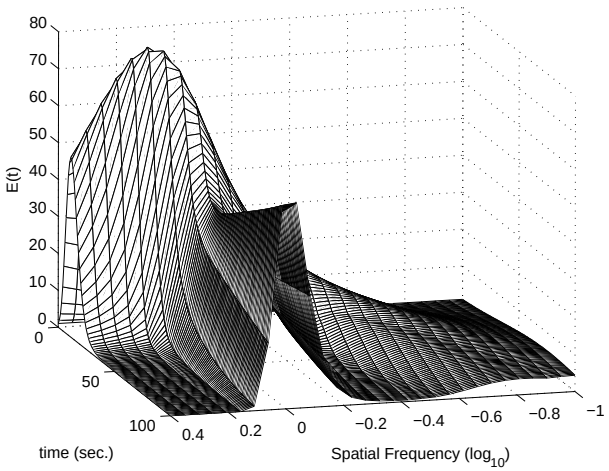

Fig. 3. $E_s(t)$ at different spatial frequencies

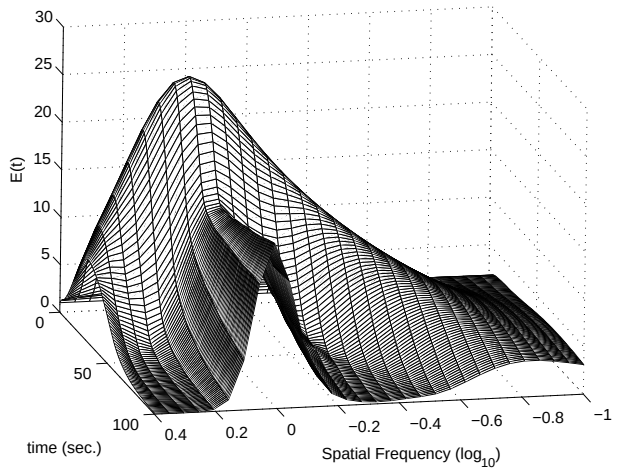

Fig. 4. $E(t)$ at different spatial frequencies for (12), using (19)

.

where

$$\begin{aligned} \Psi &= \begin{bmatrix} w_0 & & 0 \\ 0 & \ddots & 0 \\ 0 & & w_N \end{bmatrix} \\ \Lambda &= \begin{bmatrix} v_0 \\ \vdots \\ v_N \end{bmatrix}, \quad \Lambda_y = \begin{bmatrix} \frac{\partial v}{\partial y}\Big|_{y_0} \\ \vdots \\ \frac{\partial v}{\partial y}\Big|_{y_N} \end{bmatrix} \end{aligned} \tag{18}$$

In terms of the state vector (8) of the linearized model (12), (17) can be written as

$$E(t) = a^T\left(\frac{T^T\Psi T - T_y^T\Psi T_y}{4}\right)a \tag{19}$$

where T and T_y are equal to Γ and Γ' together with the deleted rows corresponding to $n = [0, 1, N-1, N]$,

respectively.

B. Results and Discussion

The transient energy for the spectral model ($E_s(t)$) - using [7] - for different spatial frequencies and $Re = 10000$ is shown in Fig 3. While the transient energy ($E(t)$) obtained for the model (12) using (19) at the same Reynolds number is shown in Fig 4. The shapes of the two surfaces is quite similar, also the values of the spatial frequencies where the two surfaces display peaks are the same. This suggests that the model (12) does capture the dominant features of the problem.

However, there are some differences as well, which should be discussed. The first difference is in the peak value. The spectral model predicts nearly three times more energy growth then the finite difference model. This means that the state transition matrix obtained from the spectral model is much more non-normal then the one obtained from finite difference approach. In fact, different discretization approaches of the same operator may result in systems having state transition matrices with different degree of normality, as shown in [11]. A second difference is the rising of the surface at zero spatial frequency in $E_s(t)$. This is due to unstable poles, which appear if the Reynolds number is increased above 5772 - these poles do not appear in the the finite difference model. However, as discussed earlier, since the phenomenon of transition from laminar flow to turbulence in plane Poiseuille flow is not due to these poles but due to the rise in transient energy, there is no significance of these poles. The third difference is the response of the system at large spatial frequencies. This is also expected as in the spectral approach a continuous space is considered, whereas in the finite difference approach we have considered discrete space.

IV. Frequency Domain Validation

In this section we compare the frequency domain results obtained from the model (12) with the results obtained from the nonlinear simulation. In order to obtain the frequency response of the system first a chain of 21 systems is created in the form of interconnected systems, as shown in Fig 5.

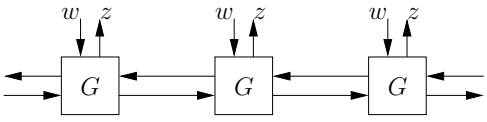

Fig. 5. Interconnected System

Then, the frequency response is found for Dirichlet boundary conditions, between input w at unit 11 and outputs z at $[1, 5, 9, 13, 16, 21]$. These are the units which are at 2, 5 and 10 sampling units away both upstream and downstream from the point of injection of disturbance. This frequency response is then compared with the response obtained from nonlinear simulation.

A. Nonlinear Simulation

In this section we present the results obtained from nonlinear simulation experiments of channel flow with moving boundary. The dynamics of the flow are modeled by the nonlinear Navier-Stokes and continuity equations , which are given as

$$\left(\frac{\partial \overline{U}}{\partial t} + \overline{U}\nabla\overline{U}\right) = -\nabla p + \mu\Delta\overline{U} \quad (20)$$

$$\nabla\overline{U} = 0 \quad (21)$$

where ∇ is the divergence operator, $\overline{U} = [U, V]^T$ is the global velocity vector, p is the pressure, μ and ρ are the viscosity and the density of the fluid, respectively.

1) Computational Domain: Since the sinusoidal input is produced by changing the profile of the lower boundary, we have a time dependent computational domain $\Omega(\psi(x,t), y)$, where ψ represents the time varying deformation of the lower boundary and is given by

$$\psi(x,t) = \begin{cases} \kappa, & \forall x \in [x_i - 0.05\delta, x_i + 0.05\delta], \\ 0, & \text{elsewhere}, \end{cases} \quad (22)$$

where $\kappa = 0.05\delta \sin(wt)\Big(1 + \cos\big(\frac{\pi(x-x_i)}{0.05\delta}\big)\Big)$. Thus, the maximum amplitude of the disturbance is 10% of the half width of the channel. It is assumed that the fluid will exhibit linear behavior within this range. This will generate the time-dependent profile of the lower boundary as shown in Fig 6.

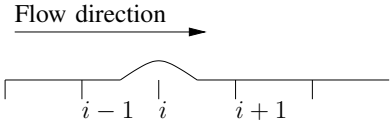

Fig. 6. Actuation at the lower boundary.

2) Initial and Boundary conditions: The initial condition used in simulation are

$$\begin{aligned} \overline{U}(x,y,t=0) &= 0 \\ p(x,y,t=0) &= 0, \\ \forall (x,y) \in \Omega & \end{aligned} \quad (23)$$

The computational domain Ω consists of four boundaries; the inflow part $\partial\Omega_{in}$, the outflow part $\partial\Omega_{out}$, the upper boundary $\partial\Omega_{up}$ and the lower moving boundary $\partial\Omega_{low}$.

The following boundary conditions are used in the simulations:

For $\partial\Omega_{in}$:

$$\begin{aligned} U(x,y,t) &= (1-y^2)U_0, \\ V(x,y,t) &= 0 \\ & \forall (x,y) \in \partial\Omega_{in}, t \in (0,T) \end{aligned}$$

where U_0 is the constant centreline velocity.

For $\partial\Omega_{out}$: Neumann boundary conditions are implemented by

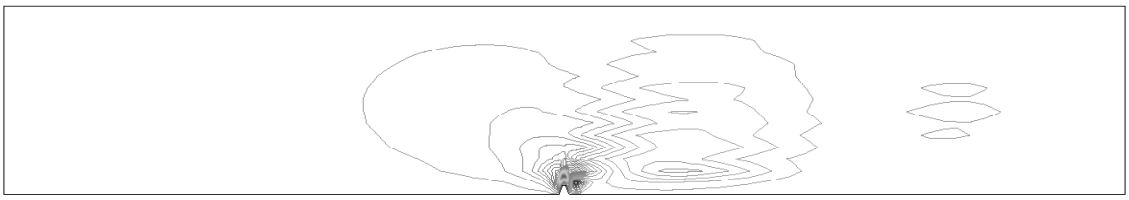

Fig. 7. Vertical velocity at $t = 8$ sec for $w = 0.2$rad.

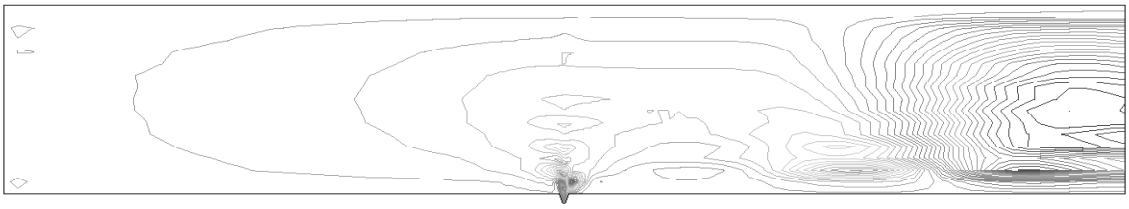

Fig. 8. Vertical velocity at $t = 24$ sec for $w = 0.2$rad.

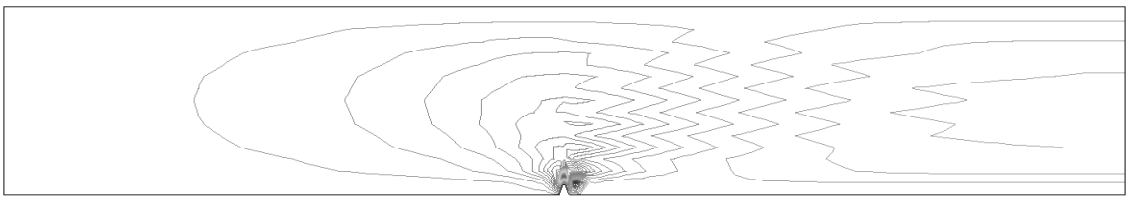

Fig. 9. Vertical velocity at $t = 156$ sec for $w = 0.01$rad.

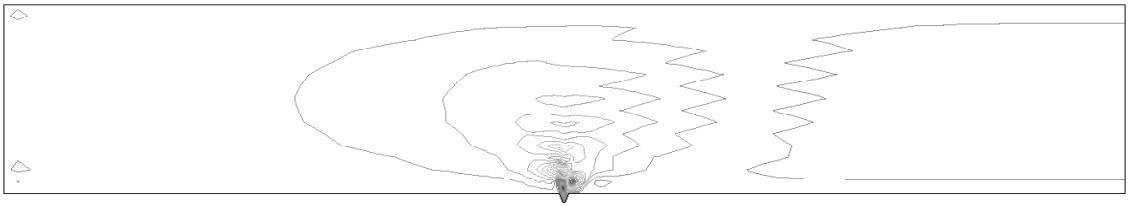

Fig. 10. Vertical velocity at $t = 470$ sec for $w = 0.01$rad.

$$\begin{aligned} \left(2\mu\frac{\partial U}{\partial x} - p\right)(x,y,t) &= 0, \\ \left(\mu\Big(\frac{\partial V}{\partial x} + \frac{\partial U}{\partial y}\Big)\right)(x,y,t) &= 0 \\ \forall (x,y) \in \partial\Omega_{out}, t \in (0,T). \end{aligned} \tag{24}$$

For $\partial\Omega_{up}$: Non-slip condition is used,

$$\begin{aligned} U(x,y,t) = 0, V(x,y,t) = 0 \\ \forall (x,y) \in \partial\Omega_{up}, t \in (0,T). \end{aligned} \tag{25}$$

For $\partial\Omega_{low}$: This boundary includes the deforming part of $\partial\Omega$. Here, the velocity of the fluid equals the velocity of the moving domain; this is modeled by

$$\begin{aligned} U(x,y,t) &= 0, \\ V(x,y,t) &= \frac{\partial\psi(x,t)}{\partial t} = V^{grid}(x,y,t), \\ &\forall (x,y) \in \partial\Omega_{low}, t \in (0,T). \end{aligned} \tag{26}$$

where V^{grid} is the velocity of the mesh movement.

3) Discretization Method: The UG software toolbox [12] is used to simulate the dynamics with the following options:

- In time, the Backward-Euler implicit method is used .
- For the space discretization, the finite volume method is used with the pseudo-compressibility stabilization as used by [13]. The nonlinear convective term is handled by the Newton method [13].
- The dual finite volume grid is obtained from the original rectangular grid using the staggered grid technique. Here, the problem is discretized on control volumes

using a piecewise constant test function. These functions approximate the velocities and pressure inside the control volume using the values at the grid point.
- An arbitrary Lagrangian Eulerian formulation is used to represent the mesh movement, as done in [14].

The wall shear force (WSF) at the lower boundary at $[2, 5, 10]\delta$ locations upstream and downstream is calculated as the output. This is defined as

$$WSF = -2\frac{1}{Re}\left(\frac{\partial^2 U}{\partial x \partial y}\right)_{y=-1}. \quad (27)$$

The simulation experiments are carried out for $Re = 10000$ and $w = \{0.01, 0.06, 0.1, 0.12, 0.13, 0.14, 0.2, 0.3, 0.5, 1\}$ rad/sec. These frequencies are chosen from the frequency response of the linearized model for which nonlinear simulation results can be obtained in reasonable computational time. Each simulation is run for two periods of ψ. Computations are started 90sec before the start of the sinusoidal signal to ensure the steady flow. During this time the lower boundary is kept stationary. Fig 9 and Fig. 10 show the velocity profiles obtained from the simulation for $w = 0.2$ rad at $t = 8, 24$ sec, when the disturbance has maximum and minimum amplitude.

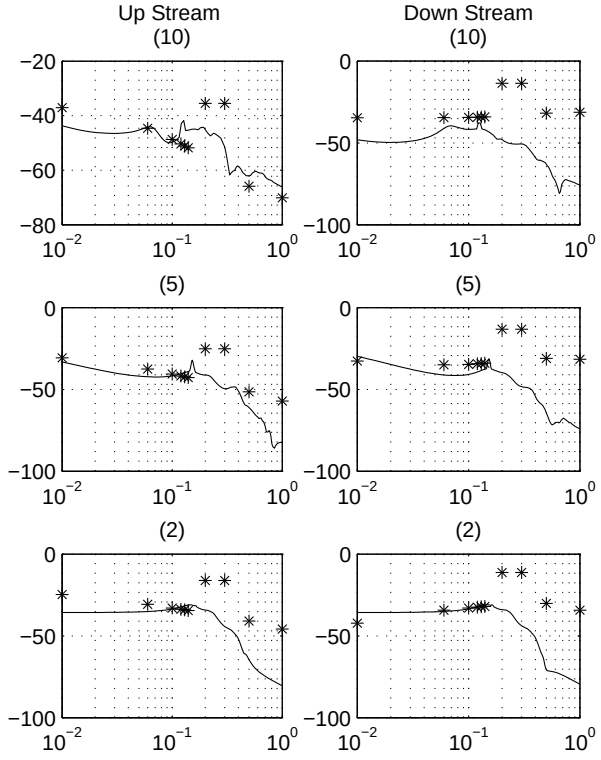

Fig. 11. Frequency response of linearized model (solid) and obtained from non-linear simulation ($*$)

Fig. 11 shows the comparison of the frequency response of the linearized and nonlinear systems at $[2, 5, 10]$ spatial sampling units upstream and downstream from the point of injection of a sinusoidal disturbance. From the figure, the following observations can be made:

- The linearized model predicts reasonably well in low frequency range both upstream and downstream.
- For frequencies above 0.15 rad/sec the deviations start to increase. This is because of the instability of the flow, which occurs in the frequency range of $[0.20.27]$rad/sec [3], and excites the nonlinear dynamics of the system. This results in deviation from the linearized model.

Moreover, the linearized frequency response ignores boundary effects. This is equivalent to considering a very long channel where a disturbance injected at one point produce a local effect. Since in the case of high Reynolds numbers this assumption is no longer valid - especially downstream - due to spatial instability of the flow, large deviations are expected in the downstream response. This can been seen in Fig 9 and 10, where the disturbance injected at $t = 8$ sec has propagated downstream at $t = 24$ sec. Furthermore, the numerical precision of the nonlinear simulation also affects the deviation, since to keep it in the linear range the magnitude of the disturbance is kept very small. Lastly we have computed only two cycles, because of the computation time and the amount of memory required. This could mean that the flow is still in its transient phase, while the frequency response of the linearized model is based on the assumption that the response is in steady state.

However, the model can be used for synthesizing robust spatially interconnected controller. since the control objective is to control this transition at the very onset: the controller should not let the flow become unstable and try to suppress the effect of disturbance at the very beginning.

V. Conclusion

Recently a new model has been proposed to design spatially interconnected controllers for transition control in plane Poiseuille flow. These controllers are easier to implement, since these are in the physical domain rather than Fourier domain, as were previously presented models. In this paper the model has been validated in both time and frequency domain for $Re = 10000$.

For time domain validation, transient energy responses for different spatial frequencies are obtained. It is found that the transient energy response from the proposed model does capture the dominant features of the problem. For frequency domain validation a nonlinear simulation experiment is developed. The simulation is run with sinusoidal disturbances of different frequencies. Results suggest that the linearized model predicts the nonlinear behaviour reasonably well. Any deviation from the linearized response is due to nonlinear effects, boundary effects or numerical precision. Although the results are only presented for $Re = 10000$, the same simulation has also been used to generate the response of the flow at different Reynolds numbers and different frequencies, leading to similar results.

REFERENCES

[1] T. Bewley, "Flow control: new challenges for a new renaissance," *Progress in Aerospace sciences*, vol. 37, no. 1, pp. 21–58, 2001.

[2] S. Orszag, "Accurate solution of the Orr-Sommerfeld stability equation," *Journal of Fluid Mechanics*, vol. 50, no. 4, pp. 689–703, 1971.

[3] S. Chughtai and H. Werner, "Transition control of plane poiseuille flow - a spatially interconnected model," in *Proceedings of the 47th IEEE Conference on Decision and Control.*, 2008.

[4] K. Butler and B. Farrell, "Three dimensional optimal disturbances in viscous shear flow," *Physics of Fluids*, vol. 4, no. 8, pp. 1637–1650, 1992.

[5] L. Trefethen, A. Trefethen, S. Reddy, and T. Driscoll, "Hydrodynamic stability without eigenvalues," *Science*, vol. 261, no. 30, pp. 578–584, 1993.

[6] J. McKernan, J. Whidborne, and G. Papadakis, "Linear quadratic control of plane Poiseuille flow-transient behaviour," *International Journal of Control*, vol. 80, no. 12, pp. 1912–1930, 2007.

[7] J. McKernan, *Control of plane Poiseuille flow: A theoretical and computational investigation*, Ph.D. thesis, Cranfield University, Dept. of Aerospace Siences, School of Engineering, 2006.

[8] R. Peyret, *Spectral methods for incompressible viscous flow*, Applied Mathematical Science. Springer, Berlin, 2002.

[9] J. Boyd, *Chebyshev and Fourier Spectral Methods*, Dover Publications Inc., NewYork, 2001.

[10] L. Trefethen, "Pseudospectra of linear operators," *SIAM Review*, vol. 39, no. 3, pp. 383–406, 1997.

[11] A. Harrabi, "On the approximation of pseudospectra of non normal operators by discretization, part 1: the first derivative operator," Tech. Rep., CERFACS, 1998.

[12] P. Bastian, K. Birkenn, K. Johannsen, S. Lang, N. Neuß, H. Rentz-Reichert, and C. Wieners, "Ug: A flexible software toolbox for solving partial differential equations," *Computing and Visualization in Science*, vol. 1, no. 1, 1997.

[13] S. Nagele and G. Wittum, "On the influence of different stabilisation methods for the incompressible Navier-Stokes equations," *Journal of Computational Physics*, vol. 224, no. 1, pp. 100–116, 2007.

[14] A. Quarteroni, "Mathematical modeling of the cardiovascular system," in *Proc. of Inter. Congress of Mathematicians*, 2002.